SOLUBILITY ENHANCEMENT OF POORLY WATER-SOLUBLE NORFLOXACIN BY ENCAPSULATION INTO SBA-15-TYPE SILICA CARRIERS

Mihaela DEACONU[1], Lucia PINTILIE[2], Raul Augustin MITRAN[3], Cristian MATEI[4], Daniela BERGER[5]

A method to improve the bioavailability of poorly water-soluble drugs is their encapsulation into carriers in amorphous state. Pristine and functionalized SBA-15 mesoporous silica with an ordered 1D hexagonal pore framework are promising carriers for various biologically active molecules encapsulation due to their biocompatibility, high porosity, and the ability to adsorb large amount of drug into their mesopores. The active pharmaceutical ingredient molecules are accommodated mainly in amorphous state into silica pore channels, because of the nano-confinement effect. Thus, by suppressing the drug crystallization energy its solubility is enhanced.

The paper presents studies on norfloxacin adsorption into pristine and functionalized SBA-15 silica supports to obtain drug delivery systems, whose behavior was investigated in vitro in simulated intestinal fluid (SIF), pH 7.4. Both SBA-15-type carriers and norfloxacin delivery systems were characterized by various techniques: FTIR spectroscopy, small- and wide-angle XRD, scanning electron microscopy and nitrogen adsorption-desorption isotherms. The norfloxacin release data proved enhanced antibiotic dissolution rate when it is encapsulated into SBA-15-type silica carriers.

Keywords: mesoporous silica, norfloxacin, drug delivery systems, poorly water-soluble drug, SBA-15 silica

1. Introduction

In the last decades, researchers have made great efforts in developing new antibiotics to fight against antimicrobial resistance, but the discovery of new molecules is a long and costly process. Therefore, the development of new

[1] PhD student, Dept. of Inorganic Chemistry, Physical Chemistry and Electrochemistry, University POLITEHNICA of Bucharest, Romania, e-mail: mihaela_deaconu@yahoo.com

[2] PhD Eng., National Institute for Chemical-Pharmaceutical Research and Development, Bucharest, Romania

[3] PhD Eng., "Ilie Murgulescu" Institute of Physical-Chemistry, Bucharest, Romania

[4] Prof., Dept. of Inorganic Chemistry, Physical Chemistry and Electrochemistry, University POLITEHNICA of Bucharest, Romania

[5] Prof., Dept. of Inorganic Chemistry, Physical Chemistry and Electrochemistry, University POLITEHNICA of Bucharest, Romania; e-mail: danaberger01@yahoo.com

formulations of the existing biologically active molecules is an approach that has gained more interest [1].

Norfloxacin (NFX) (Scheme 1) is a broad-spectrum fluoroquinolone antibiotic with good activity against Gram-positive and Gram-negative aerobic bacteria. It is primarily used in treating urinary tract infections, sexually transmitted diseases and prostatitis. NFX is slightly soluble in ethanol and acetone and practically insoluble in water [2-5]. Moreover, NFX has low lipophilicity so the molecules hardly cross the phospholipid bilayer of the cellular membrane causing low bioavailability.

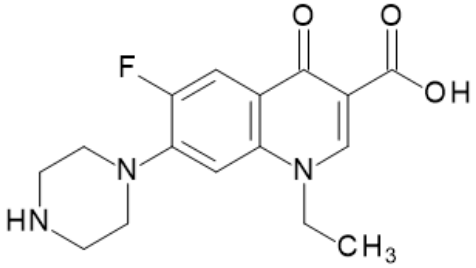

Scheme 1. Chemical structure of norfloxacin

There are different approaches to overcome the low solubility of an active pharmaceutical ingredient (API), one of the most common practices being the drug salts formation. It involves screening of different counter ions and crystallization conditions that is usually a difficult task. Moreover, the resulted drug salts could be highly hygroscopic or present lower chemical stability than the pristine drug [6,7]. Other approaches for the improved dissolution of poorly water-soluble drugs are: liquid formulations of insoluble drugs using co-solvent or surfactants, solid dispersions in which API is either in amorphous state or included in a polymer excipient, pharmaceutical cocrystal technology, polymeric micelles with low critical micellar concentration and stability in a large concentration range, complexation using cyclodextrins, nanoparticles (NPs)-based technology and microemulsion approach [8-10]. All these technologies are very laborious and are very sensitive to the API properties.

Ordered mesoporous silica nanoparticles have very interesting features that offer the possibility for their employment in the development of new drug delivery systems. SBA-15 mesoporous silica (SBA = Santa Barbara Amorphous) has an ordered hexagonal 1D pore array with large total pore volume and surface area values that allows a high drug uptake [11,12]. The biologically active molecules entrapment into mesoporous silica matrix in amorphous state is a facile method for drug water-solubility enhancement.

The API molecules are adsorbed into silica mesopores through weak interactions like hydrogen bonding or van der Waals forces. To enhance these

interactions, organic groups can be linked to the silanol groups present either on the inner or outer pore walls of the silica, resulting functionalized materials that are able to improve the pharmacokinetic properties of biologically active molecules [13,14].

Herein, we report the employment of pristine and functionalized mesoporous SBA-15 silica matrices for the dissolution rate enhancement of norfloxacin, a poorly water-soluble antibiotic. It is based on the concept that the nano-confinement of a poorly water-soluble drug in amorphous state into silica mesopores increases the drug solubility.

2. Experimental

2.1. Materials

Tetraethyl orthosilicate (TEOS, Fluka), poly(ethylene glycol)-*block*-poly(propylene glycol)-*block*-poly(ethylene glycol) (Pluronic P123, Sigma-Aldrich), hydrochloric acid 37% (Merck), methyltriethoxysilane (MTES, Sigma-Aldrich), (3-aminopropyl)triethoxysilane (APTES, Sigma-Aldrich), malonic acid (Sigma-Aldrich), N-hydroxysuccinimide (NHS, Sigma-Aldrich), N,N'-diisopropylcarbodiimide (DCDI, Sigma-Aldrich), acetonitrile (Riedel-de Haën), toluene (Riedel-de Haën), ethanol (Sigma-Aldrich), hydrogen peroxide 30% (Fluka), N,N-dimethylformamide (Merck), sodium chloride (Sigma-Aldrich), sodium hydrogen carbonate (Sigma-Aldrich), potassium chloride (Sigma-Aldrich), potassium phosphate dibasic trihydrate (Fluka), magnesium chloride hexahydrate (Sigma), calcium chloride (Sigma-Aldrich), sodium sulfate (Sigma), tris(hydroxymethyl)aminomethane (Sigma-Aldrich) were used as received. Ultrapure deionized water (Millipore Direct-Q3UV water system with Biopack UF cartridge) was used for all experiments.

Norfloxacin (NFX) was prepared at the National Institute for Chemical-Pharmaceutical Research and Development according to the synthesis route presented by Pintilie *et al.* [15]. NFX was used after recrystallization in N,N-dimethylformamide.

2.2. Synthesis of pristine SBA-15 silica carriers

Pristine SBA-15 materials were prepared through sol-gel method assisted by hydrothermal treatment. Briefly, 1.74 g block copolymer Pluronic P123 were dissolved in a mixture of 55 mL water and 9.5 mL concentrated hydrochloric acid and then 4.1 mL tetraethyl orthosilicate were added dropwise. The reaction mixture was kept under magnetic stirring for 24 h at room temperature and then hydrothermally treated at 70 ^{o}C or 100 ^{o}C. The solids were filtered off and dried at room temperature. The surfactant was removed in two-steps extraction: reflux in

ethanol followed by extraction at room temperature in a mixture of aqueous solution of 5% H_2O_2 and 0.7% HCl. The SBA-15 material hydrothermally treated at 70 ^oC and purified by extraction was labeled SBA-15(2)E. After extraction, the samples were calcined at 550 ^oC for 5 h and labeled SBA-15(1) and SBA-15(2) corresponding to hydrothermally treated materials at 100 ^oC and 70 ^oC, respectively.

2.3. Synthesis of functionalized SBA-15 silica carriers

The functionalized SBA-15 materials were obtained by either co-condensation or post-synthesis method. Thus, methyl-functionalized SBA-15 (SBA-MTES) was prepared through co-condensation using a 10:1 TEOS : MTES molar ratio and the same conditions as for SBA-15(1) material.

The amide functionalized sample (SBA-Mal) was prepared firstly by grafting amine groups on SBA-15(1) followed by condensation with malonic acid. Thus, 0.2 g SBA-15(1) were dispersed in 20 mL toluene and then a solution of 0.040 mL (3-aminopropyl)triethoxysilane (APTES) in 5 mL toluene was added. The reaction mixture was heated at reflux for 4 h and the resulted material was separated by centrifugation, washed with toluene, ethanol and 1 M HCl, and dried at room temperature (the sample was labeled SBA-APTES). Further, for the condensation reaction, 0.15 g SBA-APTES were dispersed in 5 mL equimolar solution of malonic acid, N-hydroxysuccinimide, N,N'-diisopropylcarbodiimide in acetonitrile, considering a 1 : 1.5 molar ratio between aminopropyl moieties and malonic acid. The reaction mixture was kept under magnetic stirring, at room temperature for 18 h, and the solid was filtered off, washed with acetonitrile, water and ethanol, and then dried at room temperature.

2.4. Characterization of materials

The materials were characterized by N_2 adsorption-desorption isotherms at 77 K (Quantachrome Autosorb iQ_2 surface area and pore size analyzer analyzer, Quantachrome Instruments). The specific surface area values were determined with Brunauer-Emmett-Teller (BET) method and the pore size distribution curves were computed using Barrett-Joyner-Halenda (BJH) model from the desorption branch of the corresponding isotherm. Small-angle X-ray diffraction (XRD) analyses were performed in the 2θ range of 0.5 - 3^o, with a scanning rate of 0.5 ^{o}/min and 0.02 ^{o}/step (Bruker B8 Discover diffractometer with Cu-Kα radiation, λ = 1.5406 Å), while wide-angle XRD patterns were recorded in the range of 2θ, 10 - 50^o, with a scanning rate of 2 ^{o}/min (Rigaku Miniflex II diffractometer with Cu-Kα radiation, λ = 1.5406 Å). FTIR spectroscopy was performed using KBr pellet technique in the 4000 – 400 cm^{-1} wavenumber range on a Bruker Tensor 27 spectrometer. The morphology of SBA-15-type materials was investigated by

scanning electron microscopy (SEM) using a Tescan Vega 3 LMH microscope. Thermogravimetric analyses were performed to determine the content of organic moieties bonded on the silica pore walls on a Mettler Toledo TGA/SDTA 851e equipment under air flow, in the temperature range 20-1000 ^{o}C, with a 10 ^{o}C/min heating rate.

2.5. Preparation of drug-loaded materials

Norfloxacin-loaded materials (denoted NFX@*carrier*) were obtained by incipient wetness impregnation method. The drug-loaded materials with 20% (wt) drug content were obtained by addition of the corresponding volume of 3 mg/mL NFX solution in 1-propanol to 0.1 g carrier, followed by solvent evaporation in vacuum for 12 h. SBA-15(1) carrier was also loaded with 30% (wt) drug content in resulted composite material to study the influence of norfloxacin amount on the antibiotic release kinetics. This sample was denoted NFX30@SBA-15(1).

2.6. *In vitro* drug release studies

NFX release experiments were performed in pH 7.4 simulated intestinal fluid (SIF) prepared according to literature data [16] in dark conditions, at 37 ^{o}C, under constant magnetic stirring. Depending on the drug content in NFX-loaded sample, the appropriate amount of NFX@carrier sample containing 8 mg NFX was suspended in 90 mL SIF. At set time intervals, 1.5 mL suspension were withdrawn from the release fluid, centrifuged and 0.1 mL supernatant was diluted and analyzed by UV-Vis spectroscopy (λ_{max} = 273 nm). The remainder of the centrifuged suspension was redispersed and reintroduced into the release medium.

3. Results and discussion

3.1. Characterization of supports

To obtain norfloxacin delivery systems, firstly the SBA-15-type carriers were synthesized and characterized by small-angle XRD, FTIR spectroscopy and N_2 adsorption-desorption isotherms. All materials present a highly ordered hexagonal pore array evidenced in their small-angle XRD patterns (Fig. 1 A) by the presence of the intense (100) peak and the two smaller (110) and (200) Bragg reflections. One can notice that the functionalization of pristine silica does not alter the ordered mesophase, but the (100) Bragg reflection is shifted towards higher 2θ values (lower d_{100}-spacing values) due to the presence of the organic moieties linked on the silica pore walls surface, which leads to the narrowing of pore channels for functionalized materials in comparison with the pristine one.

The carriers' functionalization was demonstrated by FTIR spectroscopy (Fig. 1 B). All FTIR spectra showed the specific vibrations of silica matrix corresponding to Si–O–Si (1082, 806 and 470 cm^{-1}) and Si–OH (960 cm^{-1}) bonds. The C–H stretching vibrations from 2860-2980 cm^{-1} correspond to the methyl groups grafted on silica pore walls of SBA-MTES material. The shoulder at 3070 cm^{-1} shows the successful grafting of aminopropyl groups on the silica surface. In the case of SBA-Mal material, the amide group band overlaps with the vibration of physically adsorbed water from 1630 cm^{-1}, but it is more intense in comparison with that of SBA-APTES.

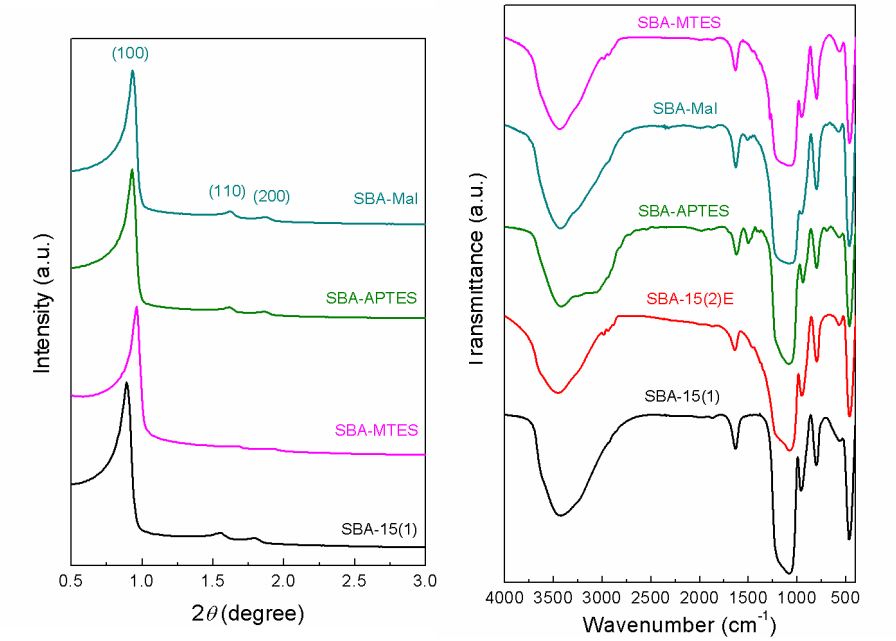

Fig. 1. Small-angle XRD (A) and FTIR spectra (B) of SBA-15-type carriers

The organic moieties content was determined through thermogravimetric analysis (TG-DTA) (Fig. 2) in the 125-1000 ^{o}C temperature range, without considering the weight loss associated to the first endothermic effect up to 110 ^{o}C, which is owed to the loss of adsorbed water molecules. The condensation yield of malonic acid with the amine groups grafted on the silica was computed from the TG-DTA analysis (Fig. 2 A) after determining the amount of the amine groups (TG analysis not shown). The resulted molar ratio for SiO_2 : amine groups was 1:0.12 (10.7% organic mass loss) and for SiO_2 : amide groups was 1:0.06 corresponding to a 12.6% mass loss. The TG-DTA analysis of SBA-MTES (Fig. 2 B) shows a 10.5% organic mass loss equivalent to a SiO_2 : methyl groups molar ratio of 1:0.47.

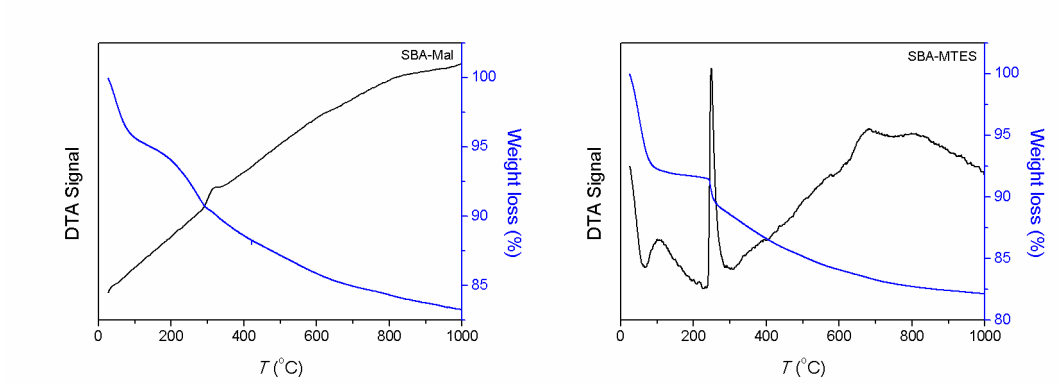

(A) **(B)**

Fig. 2. Thermal analyses of SBA-Mal (A) and SBA-MTES (B)

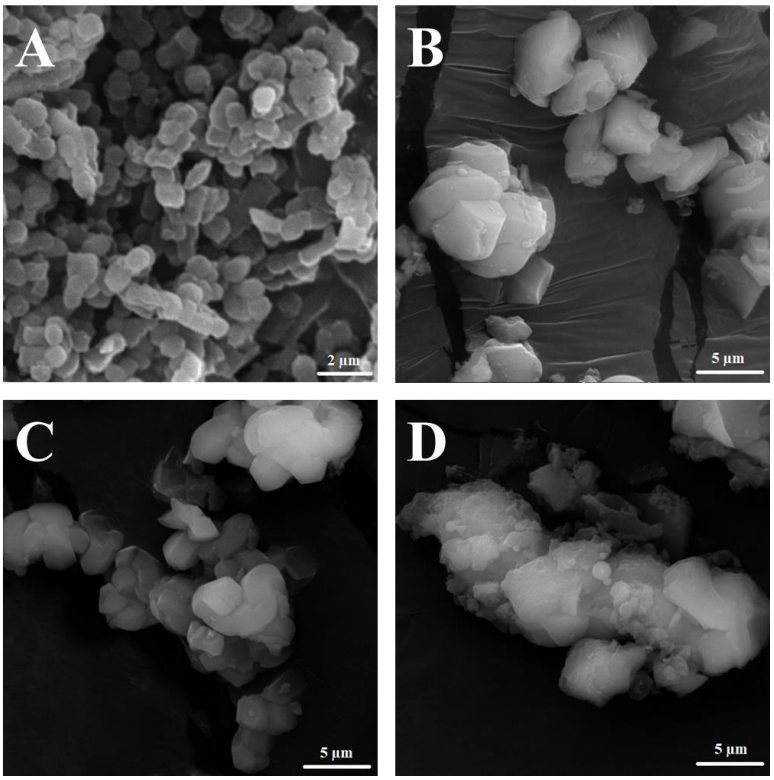

Fig. 3. SEM micrographs of SBA-15 materials:
(A) SBA-15(1), (B) SBA-15(2)E, (C) SBA-Mal, (D) SBA-MTES

In Fig. 3 one can observe the SEM images of SBA-15-type carriers. Pristine SBA-15(1) material consists of round-shaped particles with a diameter up to 1 µm, with uniform size distribution (Fig 3 A). When hydrothermal treatment was performed at lower temperature (70 ^{o}C), larger particles with irregular shape

and tendency to aggregate resulted (Fig 3 B). The post-synthesis functionalization did not influence the morphological features of the material as it can be seen in the case of SBA-Mal (Fig. 3 C), while the sample obtained by co-condensation, SBA-MTES, exhibits particles with irregular shape and size (Fig. 3 D).

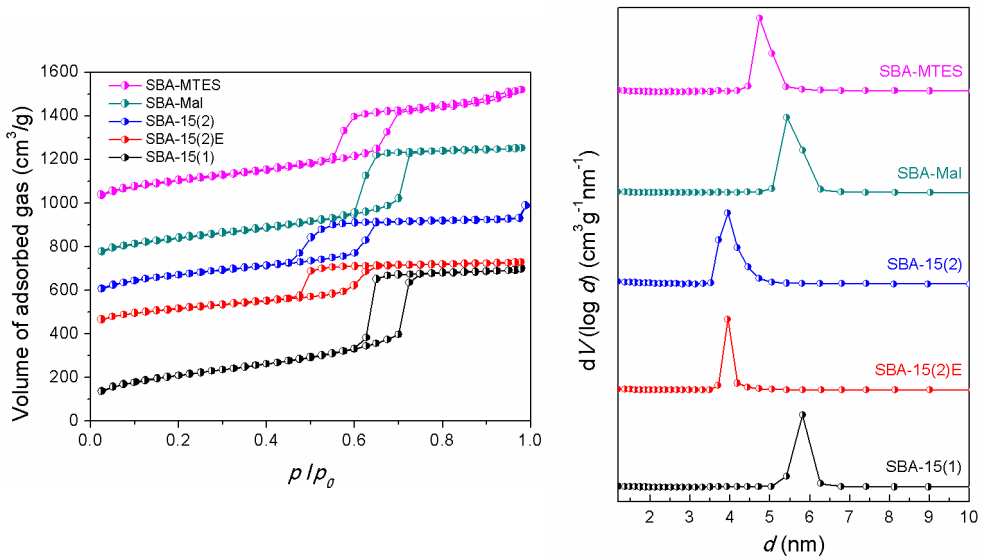

Fig. 4. Nitrogen adsorption-desorption isotherms (left) and the corresponding pore size distribution curves (right) of SBA-15-type supports

Table 1

Structural and textural properties of carriers

Sample	S_{BET} (m^2/g)	V_p (cm^3/g)	d_{BJH} (nm)
SBA-15(1)	748	1.11	5.82
SBA-15(2)E	506	0.58	3.94
SBA-15(2)	712	0.81	3.94
SBA-Mal	595	0.94	5.42
SBA-MTES	631	0.96	4.74

All pristine and functionalized samples exhibit type IV nitrogen adsorption-desorption isotherms (Fig. 4-left) characteristic for mesoporous materials [17] with hysteresis loop and completely reversible in the relative pressure range of 0-0.45 and 0-0.6 for SBA-15 samples hydrothermally treated at 70 ^oC and 100 ^oC, respectively. The unimodal pore size distribution curves (Fig. 4-right) were computed with Barrett-Joyner-Halenda model and the specific surface area values were determined in the relative pressure range of 0-0.30 using

BET method. The temperature of hydrothermal treatment for SBA-15 materials influences their textural properties. Thus, a lower temperature leads to smaller average pore size (3.94 nm versus 5.82 nm) and a decreased porosity (lower specific surface area and total pore volume values). As expected, the introduction of organic moieties either through co-condensation or post-synthesis procedure induces the decrease of average pore size, specific surface area and total pore volume values (Table 1).

3.2. Characterization of NFX-loaded materials

The structural and textural properties of prepared norfloxacin-loaded samples were investigated by wide-angle XRD, FTIR spectroscopy and N_2 adsorption-desorption isotherms. No crystalline phase of NFX was observed in the case of drug-loaded pristine SBA-15 samples with 20% (wt.) drug into composite material (Fig. 5 A). Higher drug content in norfloxacin-loaded pristine SBA-15 (30% wt) determined a partial crystallization of the antibiotic, evidenced in wide-angle XRD pattern (Fig. 5 A). The functional groups bonded on silica pore walls surface also led to a crystallization of NFX. The antibiotic presence into the pores of the mesostructured SBA-15-type carriers was demonstrated by FTIR spectroscopy. NFX characteristic vibration bands [18] at 2950 cm^{-1} corresponding to aromatic C-H stretching, 1720 cm^{-1} assigned to the carbonyl stretching vibration, and 1475-1480 cm^{-1} stretching vibration correlated with the O-C-O bond from the acid group are present on the FTIR spectra of all samples, regardless to the drug content into the composite sample (Fig. 5 B).

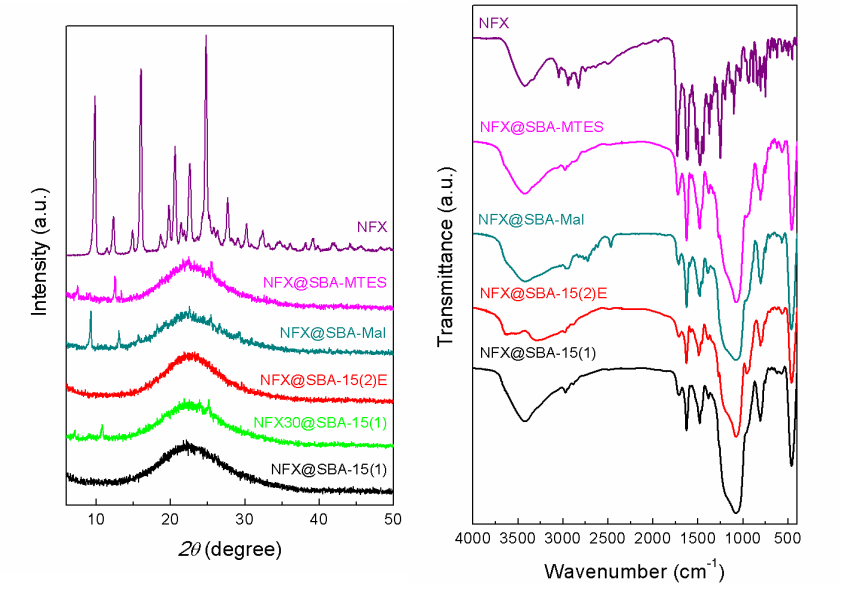

(A) **(B)**

Fig. 5. Wide-angle XRD (A) and FTIR spectra (B) of NFX-loaded carriers

The presence of antibiotic molecules into the carrier mesopores was evaluated by nitrogen adsorption-desorption isotherms. The drug-loaded materials exhibited a decreased porosity compared to the corresponding support, but the samples still showed free porosity with unimodal pore distribution curves, with average pore diameter lower than the supports (Fig. 6 and Table 2).

Table 2

Structural and textural properties of NFX-loaded carriers

Sample	S_{BET} (m^2/g)	V_p (cm^3/g)	d_{BJH} (nm)
NFX@SBA-15(1)	373	0.70	5.42
NFX30@SBA-15(1)	294	0.54	5.42
NFX@SBA-15(2)E	131	0.20	3.72
NFX@SBA-Mal	317	0.67	5.43
NFX@SBA-MTES	236	0.47	4.18

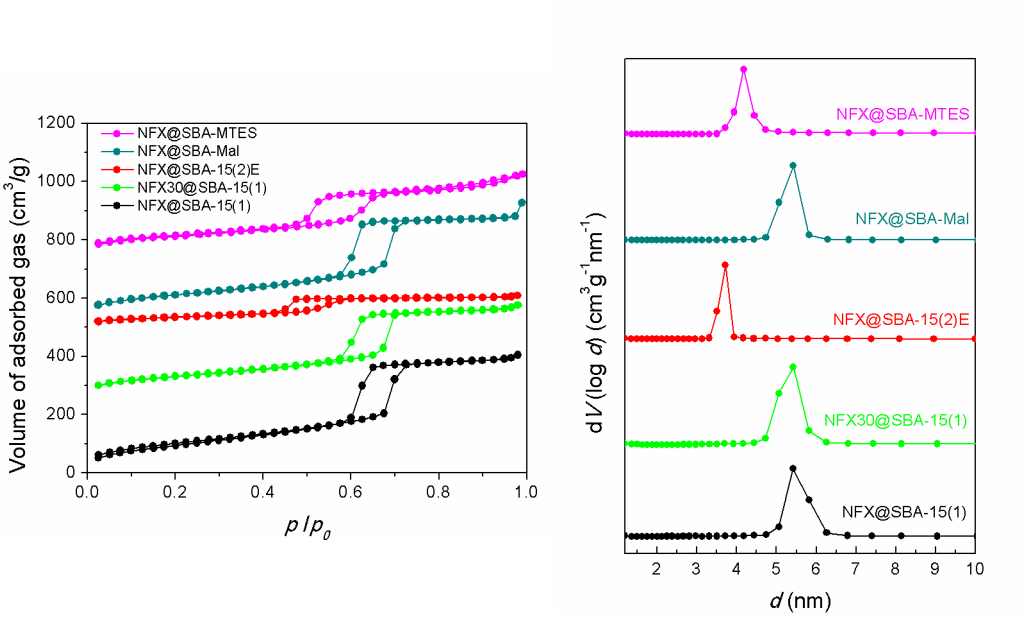

Fig. 6. Nitrogen adsorption-desorption isotherms of NFX-loaded samples (left) and their pore size distribution curves (right)

3.3. Norfloxacin release profiles from SBA-15-type carriers

Fitting drug release data is important for understanding the biologically active molecules transport mechanism in drug delivery applications. There are

several mathematical models intensively used to describe drug delivery kinetics: Higuchi, first order kinetics, Weibull function and Korsmeyer-Peppas model [19-22].

The drug release experiments were performed in intestinal simulated fluid pH 7.4. The cumulative NFX release versus time can be seen in Fig. 7. The experimental data collected at set time intervals are presented with symbols and the line represents the corresponding fitting of each data set with the three-parameter model. The results revealed that all NFX-loaded carriers showed an increased solubility exhibiting a type I release profile as classified by Ye *et al.* [23]. The experimental data of norfloxacin release profiles (Fig. 7) were fitted using a three-parameter equation (eq. 1) [24] with good correlation coefficients (in all cases, R^2>0.99).

In the three-parameter model (eq. 1) the diffusion process and the dissociation-association equilibrium between drug molecules and carrier are considered.

$$\frac{m(t)}{m(0)} = \frac{\lambda_2(k_s-\lambda_2)}{(k_{on}+k_{off})(\lambda_1-\lambda_2)}\left(1-e^{-\lambda_1 t}\right)+\frac{\lambda_1(\lambda_1-k_s)}{(k_{on}+k_{off})(\lambda_1-\lambda_2)}\left(1-e^{-\lambda_2 t}\right), \quad (1)$$

where *m(t)* and *m(0)* are the cumulative drug release at time *t* and total amount of drug in composite material, respectively; k_s is the rate constant for the diffusion process; k_{on} is the rate constant for association; k_{off} is the rate constant for dissociation; $\lambda_{1,2}$ (eq. 2) are the negative eigenvalues of the linear system used to resolve eq. 1. The free energy difference between free and bound states, ΔG (eq. 3), shows the significance of the burst release stage in the release profile, where k_B is Boltzmann's constant ($1.3806\cdot10^{-23}$ J/K) and *T* is the considered temperature (310 K).

$$\lambda_{1,2} = \frac{\left[(k_s+k_{on}+k_{off}) \pm \sqrt{(k_s+k_{on}+k_{off})^2-4k_s k_{off}}\right]}{2}, \quad (2)$$

$$\Delta G = -k_B T \ln\frac{k_{on}}{k_{off}}, \quad (3)$$

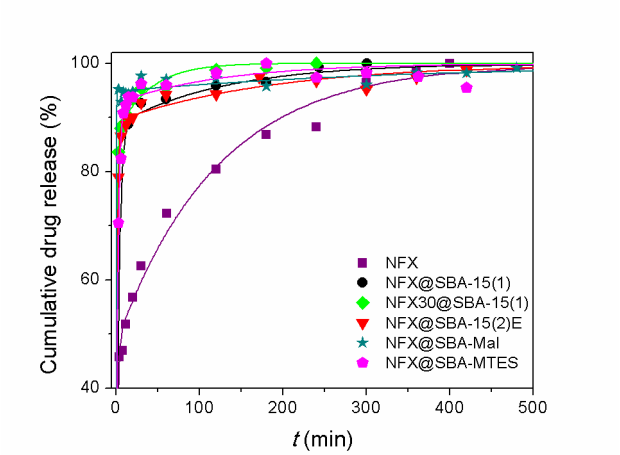

Fig. 7. Drug release profiles of NFX from SBA-15-type carriers

The rate constant values for NFX-loaded SBA-15-type supports and the correlation coefficients are presented in Table 3. The amount of free and bound drug in the initial burst stage is proportional with ΔG parameter. In case of all drug-loaded samples the free energy parameter values are positive, which indicate weak interactions between biologically active molecules and carrier. These results are correlated with the $k_{off} > k_{on}$ inequality, as dissociation is the dominant process. Slightly higher ΔG values were obtained for the functionalized SBA-15 carriers, which show the highest amount of drug released in the burst stage.

The k_s parameter offers information about the NFX diffusion rate during the burst stage. Lower drug content in the composite material leads to a slightly slower release rate in the first stage (i.e. only 2% cumulative drug release).

When pristine carriers were employed, 90% of the loaded drug content was solubilized in the first 15-20 min. For SBA-Mal support, almost instant solubilization of the antibiotic was observed, when in 3 minutes 95% of the total drug content was released.

Table 3

Kinetic parameters of the fitted experimental release data

Sample	$\Delta G \times 10^{21}$ (J)	$k_{off} \times 10^3$ (min^{-1})	$k_{on} \times 10^3$ (min^{-1})	k_s (min^{-1})	R^2
NFX	-	-	-	0.5554	0.9930
NFX@SBA-15(1)	8.98	7.91	0.97	0.2952	0.9985
NFX30@SBA-15(1)	8.26	26.2	3.80	1.0126	0.9977
NFX@SBA-15(2)E	9.16	5.28	0.62	0.7000	0.9974
NFX@SBA-Mal	12.4	2.69	0.15	3.6170	0.9980
NFX@SBA-MTES	11.0	7.98	0.62	0.4424	0.9938

6. Conclusions

Mesostructured SBA-15-type silica materials were used for the solubility enhancement of norfloxacin, a poorly water-soluble antibiotic with low bioavailability. Pristine and methyl- or amide-functionalized SBA-15 materials were prepared, characterized by XRD, FTIR spectroscopy and N_2 adsorption-desorption isotherms and employed as carriers for norfloxacin. The adsorption of norfloxacin mainly in amorphous state into all studied SBA-15-type materials improves its solubility. Slightly higher NFX release rate was observed in the burst stage when functionalized carriers were used, with an almost instant solubilization in the case of amide-functionalized material (SBA-Mal). It was demonstrated that the release kinetics is not significantly influenced by the high drug content, which instead determines a partial crystallization of the drug.

R E F E R E N C E S

[1]. *H. D. Williams, N. L. Trevaskis, S. A. Charman, R. M. Shanker, W. N. Charman, C. W. Pouton and C. J. H. Porter*, "Strategies to address low drug solubility in discovery and development", in Parmacol. Rev., **vol. 65**, no. 1, 2013, pp. 315-499

[2]. *B Holmes, R. N. Brogden and D. M. Richards*, "Norfloxacin – A review of its antibacterial activity, pharmaceutical properties and therapeutic use" in Drugs, **vol. 30**, no. 6, 1985, pp. 482-513

[3]. *** Merck Sharp & Dohme (Italia), Tablets NOROXIN® (Norfloxacin), Sept. 2008, https://www.accessdata.fda.gov/drugsatfda_docs/label/2008/019384s052lbl.pdf

[4]. *C. Mazuel*, "Norfloxacin", in Analytical Profiles of Drug Substances, K. Florey (Ed.), **vol. 20**, Academic Press, Inc, 1991, pp. 557-600

[5]. *L. Chierentin and H. R. Nunes Salgado*, "Review of properties and analytical methods for the determination of norfloxacin", in Crit. Rev. Anal. Chem., **vol. 46**, no. 1, 2016, pp. 22-39

[6]. *J. S. Reddy, S. V. Ganesh, R. Nagalapalli, R. Dandela, K. A. Solomon, K. A. Kumar, N. R. Goud and A. Nangia*, "Fluoroquinolone salts with carboxylic acids", in J. Pharm. Sci., **vol. 100**, no. 8, 2011, pp. 3160-3176

[7]. *Y. Xu, L. Jiang and X. Mei*, "Supramolecular structures and physicochemical properties of norfloxacin salts", in Acta Cryst. B, **vol. 70**, no. 4, 2014, pp. 750-760

[8]. *S. Kalepu and V. Nekkanti*," Improved delivery of poorly soluble compounds using nanoparticle technology: a review", in Drug Deliv. Transl. Res., **vol. 6**, no. 3, 2016, pp. 319–332

[9]. *V. Nekkanti and J. Rueda*, "Nanoparticles for improved delivery of poorly soluble drugs", in J. Drug, **vol. 1**, no. 1, 2016, pp. 18-27

[10]. *B. Siddalingappa, V. Nekkanti and G. V. Betageri*, "Insoluble drug delivery technologies: review of health benefits and business potentials", in OA Drug Design & Delivery, **vol. 1**, no. 1, 2013, pp. 1-5

[11]. *V. F. Vavsari, G. M. Ziarani and A. Badiei*, "The role of SBA-15 in drug delivery", in RSC Adv., **vol. 5**, no. 111, 2015, pp. 91686-91707

[12]. *C. Comanescu and C. Gura*n, "Influence of NaCl addition on the synthesis of SBA-15 mesoporous silica", U.P.B. Sci. Bull., Series B, **vol. 73**, no. 4, 2011, pp. 95-104

[13]. *V. Mamaeva, C. Sahlgren and M. Lindén*," Mesoporous silica nanoparticles in medicine. Recent advances", in Adv. Drug Deliv. Rev., **vol. 65**, no. 5, 2013, pp. 689–702

[14]. *D. Tarn, C. E. Ashley, M. Xue, E. C. Carnes, J. I. Zink and C. J. Brinker*, "Mesoporous silica nanoparticle nanocarriers: biofunctionality and biocompatibility", in Acc. Chem. Res., **vol. 46**, no. 3, 2013, pp. 792–801

[15]. *L. Pintilie, C. Negut, C. Oniscu, M. T. Caproiu, M. Nechifor, L. Iancu, C. Ghiciuc and R. Ursu*, "Synthesis and antibacterial activity of some novel quinolones", in Rom. Biotechnol. Lett., **vol. 14**, no. 5, 2009, pp. 4756-4767

[16]. *M. R. C. Marques, R. Loebenberg and M. Almukainzi*, "Simulated biological fluids with possible application in dissolution testing", in Dissolut. Technol., **vol. 18**, no. 3, 2011, pp. 15-28

[17]. *** IUPAC Recommendations, Pure & Appl. Chem., **vol. 57**, no. 4, 1985, pp. 603-619

[18]. *S. Sahoo, C. K. Chakraborti, S. C. Mishra, U. N. Nanda and S. Naik*, "FTIR and XRD investigations of some fluoroquinolones", in Int. J. Pharm. Pharm. Sci., **vol. 3**, no. 3, 2011, pp. 165-170

[19]. *J. Siepmann and F. Siepmann*, "Mathematical modeling of drug delivery", in Int. J. Pharm., **vol. 364**, no. 2, 2008, pp. 328-343

[20]. *N. A. Peppas and B. Narasimhan*, "Mathematical models in drug delivery: How modeling has shaped the way we design new drug delivery systems", in J. Control Release, **vol. 190**, 2015, pp. 75-81

[21]. *J. Siepmann and N. A. Peppas*, "Higuchi equation: Derivation, applications, use and misuse", in Int. J. Pharm., **vol. 418**, no. 1, 2011, pp. 6-12

[22]. *M. Ignacio, M. V. Chubynsky and G. W. Slater*, "Interpreting the Weibull fitting parameters for diffusion-controlled release data", in Physica A, **vol. 486**, 2017, pp. 486-496

[23]. *M. Ye, S. Kim and K. Pars*, "Issues in long-term protein delivery using biodegradable microparticles", in J. Control Release, **vol. 146**, no. 2, 2010, pp. 241-260

[24]. *L. Zeng, L. An and X. Wu*, "Modelling drug-carrier interaction in the drug release from nanocarriers", in J. Drug Delivery, **vol. 2011**, Article ID 370308, 2011